A Fully Embedded 60-GHz Novel BPF for LTCC System-in-Package Applications

Young Chul Lee, *Member, IEEE*, and Chul Soon Park, *Member, IEEE*

***Abstract*—In this paper, a novel LTCC stripline (SL) 60–GHz band-pass filter (BPF) composed of transitions to coplanar waveguide (CPW) pads for monolithic microwave integrated circuit integration is presented. For low-loss interconnection with active devices, a CPW-to-SL vertical via transition integrating air cavities and a CPW-to-CPW planar transition using internal ground planes are proposed and implemented. The fabricated transition shows an insertion loss of 1.6 dB and a reflection loss below −20 dB at the passband of the filter. The implemented SL BPF using dual-mode patch resonators shows a center frequency of 60.4 GHz, 3.5 % bandwidth, and reflection losses below −15 dB at the passband. Excluding the insertion loss of the transitions, the filter insertion loss reveals 4.0 dB.**

***Index Terms*—Bandpass filter, low-temperature cofired ceramics (LTCCs), patch rasonator, stripline.**

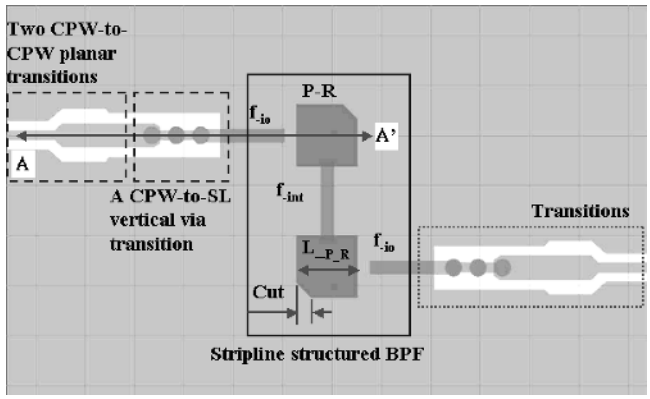

Fig. 1. Layout of a 60-GHz stripline LTCC BPF (1.8×3.5 mm^2) and transitions (2.4×0.9 mm^2) involving CPW-to-SL stagger via transitions embedding air cavities and CPW-to-CPW planar transitions for RF system integration applications (P-R: a patch resonator, f_io: an input and output feed line and f_int: an inter coupling feed line).

I. Introduction

As DEMANDS for high-speed multimedia data communications are on the rise, carrier frequencies are also increasing from low-frequency bands such as 2.4- and 5-GHz band to millimeter-wave (mm-wave) bands. Recently, many mm-wave systems, including mm-wave video transmission, wireless-LANs, and wireless Ethernets, have been proposed and developed [1]–[4]. In particular, 60-GHz band systems are very attractive because of their unlicensed wide frequency bands. In order to implement these wireless communication systems commercially, a small size and lightweight radio transceiver is indispensable. Multilayer low-temperature cofired ceramic (LTCC)-based system-in-package (SiP) technology [1]–[4], integrating monolithic microwave integrated circuits (MMICs) and passive devices, is one of the best solutions for mm-wave radio integration due to its low loss, integration capability, similar temperature coefficient of expansion (TCE) value to MMICs, and cost effectiveness.

For compact transceiver applications, the key component, especially the bandpass filter (BPF) which covers significant space and cannot be integrated within the active circuit, is required to be integrated three-dimensionally (3-D) with active circuits. In general, the BPFs have been implemented using planar structures. However, planar circuits are usually bulky and suffer from radiation of resonators and high-resonator loss. Also, integration capability is poor and an additional package is required. Special types of filter, using microelectromechanical systems (MEMS) technology [5], achieved good performance. However, the packaging and system integration issue still remain. A flip-chip type of planar dielectric waveguide filter, $4.7 \times 3.2 \times 0.25$ mm^3 in size [6], was reported for RF SiP applications [1]. For suppression of the coupling effects due to radiation, this filter was packaged as bulky as $13 \times 10 \times 1.27$ mm^3. This approach resulted in increased return losses and bulky systems.

In this paper, a novel low-radiation SL BPF, which can be fully integrated in LTCC SiP module, is presented for 60-GHz wireless communication applications. In order to fully integrate it into a LTCC SiP, a novel coplanar waveguide (CPW)-to-SL vertical transition and a CPW-to-CPW planar transition are newly devised using embedded air cavities, stagger via structures (STVs), and internal ground planes. For compact, reduced process sensitive, and low-loss filter design, the BPF is designed and implemented using dual-mode patch resonators in the LTCC dielectric.

II. Design of a Fully Embedded Stripline BPF

Miniaturization, electromagnetic interference, low-loss interconnection, and reduced process sensitivity have been considered as the most important issues for RF system integration. The miniaturization of the filter is pursued through vertical deployment of its elements using multilayer dielectrics. An electromagnetic crosstalk due to radiation has been dealt with by using a low-radiation filter and a low-loss transition structure. High fabrication tolerances of LTCC technology strongly affect poor

Manuscript received July 26, 2005; revised March 27, 2006. This work was supported by the Ministry of Science and Technology of Korea and KISTEP.

Y. C. Lee is with the Division of Marine Electronics and Communication Engineering, Mokpo National Maritime University (MMU), Mokpo, Jeonnam 530-729, Korea.

C. S. Park is with the Intelligent Radio Engineering Center, Information and Communications University (ICU), Daejeon 305-714, Korea.

Digital Object Identifier 10.1109/TADVP.2006.884807

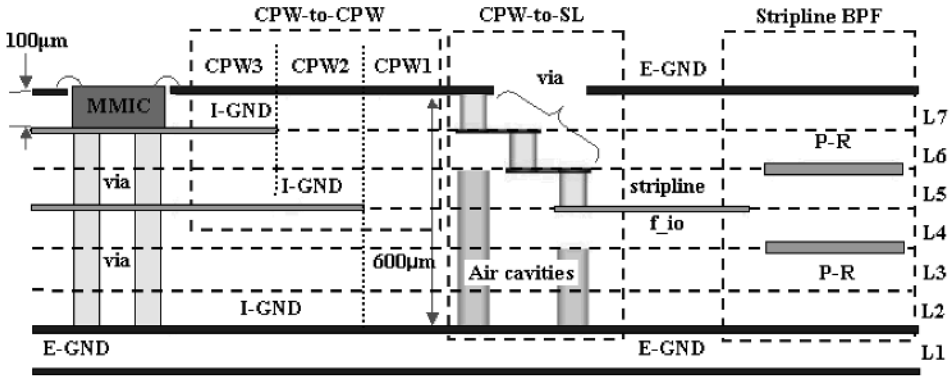

Fig. 2. Cross-sectional view of a proposed SL BPF involving two blocks at the part A-A' of Fig. 1 (E-GND: external ground plane, I-GND: internal ground plane, and Lx: number of layers).

frequency response and the repeatability of the filter. Therefore, a filter structure utilizing wide lines and widths should be proposed.

In order to meet these requirements, an SL BPF using a dual-mode patch resonator is the most preferable solution, because dispersion and radiation of a SL are negligible and upper and lower ground planes provide effective shielding. The dual-mode patch resonator offers a very compact structure because of dual-modes per resonator and an insensitiveness to process tolerances because of wide patches [7]. However, because an SL is basically a buried device, a low-loss vertical via transition is required for interconnection between a BPF and other circuits on the surface. Fig. 1 shows a fully embedded SL structured dual-mode BPF involving three transitions at each port; a novel CPW-to-SL vertical via transition and two CPW-to-CPW planar transitions. Fig. 2 shows a cross-sectional view of a proposed BPF at the part A-A' of Fig. 1. The filter and transition are vertically integrated in the multilayer LTCC.

A. Novel CPW-to-SL Vertical Via Transition Design

In the 3-D integrated radio modules, discontinuities at a CPW-to-SL transition for interconnection of embedded passive devices with surface circuits generate significant amounts of radiation as well as reflection, because the maximum dimension of the vertical vias block is more than one tenth of the wavelength $(\lambda_{\rm op})$.

In this paper, a new STV structure and embedded air cavities [8]–[10] are proposed as shown in Fig. 3 for reduction of structural discontinuities and confinement of electromagnetic (EM) fields around the transition region, respectively. In addition, the air cavities lead to reduce the parasitic additional shunt capacitance due to the STV structure. The STV structure consists of three-stacked vias through the fifth and seventh layers. These three vias are connected through lines, and their width $(W_{\rm \_TR})$ and length $(L_{\rm \_TR})$ are 100 and 107 μm, respectively. The STV is 135 μm in diameter. For confinement of EM field, the air cavities are inserted through the second to fifth layers below the seventh layer via and the second to third layers below the fifth layer via, respectively. Their optimum diameter is 170 μm. CPWs are placed on the top layer and the SL is placed on the fourth layer. In order to maintain the characteristic impedance of 50 Ω for both CPWs and the SL, the width (W1) and gap (G1) of the

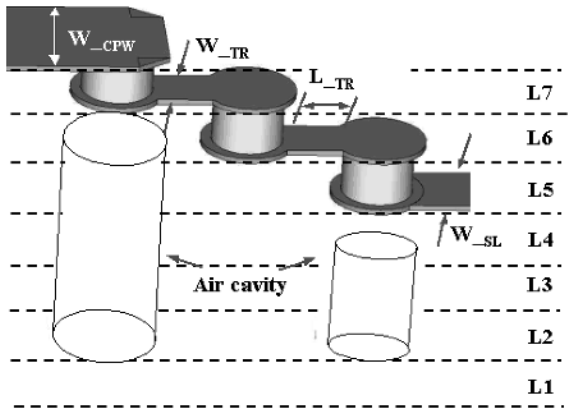

Fig. 3. Novel CPW-to-SL vertical via transition.

CPWs are 244 and 100 μm, respectively, and the SL is 135 μm in width $(W_{\rm \_SL})$.

Using the 3-D finite integration technique (FIT) simulator [11], the proposed novel transition is designed in seven LTCC dielectric layers. Their dielectric constant and loss tangent (tan δ) are 7.0 and 0.009, respectively, at 60 GHz and the thickness between the metal layers is 100 μm. The internal and external conductors are Ag and Ag/Pd, respectively. We design two three-segment transmission lines (CPW-SL-CPW) using the proposed CPW-to-SL vertical transition (a length of CPW $=$ 350 μm and that of SL $=$ 2000 μm) shown in Fig. 3 and the conventional one (a length of CPW $=$ 335 μm and that of SL $=$ 2595 μm) with directly stacked vias. Reduction in radiation due to structural discontinuities is investigated.

Fig. 4 shows the electric field distribution of each via transition region in two three-connected transmission lines. The amount of radiation can be roughly quantified by noting the extent of light blue, green, yellow, and red away from the vertical vias. In Fig. 4(b), it is seen that electric fields are better confined than the conventional one. These electric field confinements can lead to improve the transmission characteristics of the transition.

Fig. 5 presents the simulated transmission coefficients of two three-part transmission lines using the proposed transition and the conventional one. In the case of the three-segment transmission line using the novel transition, as expected from elec-

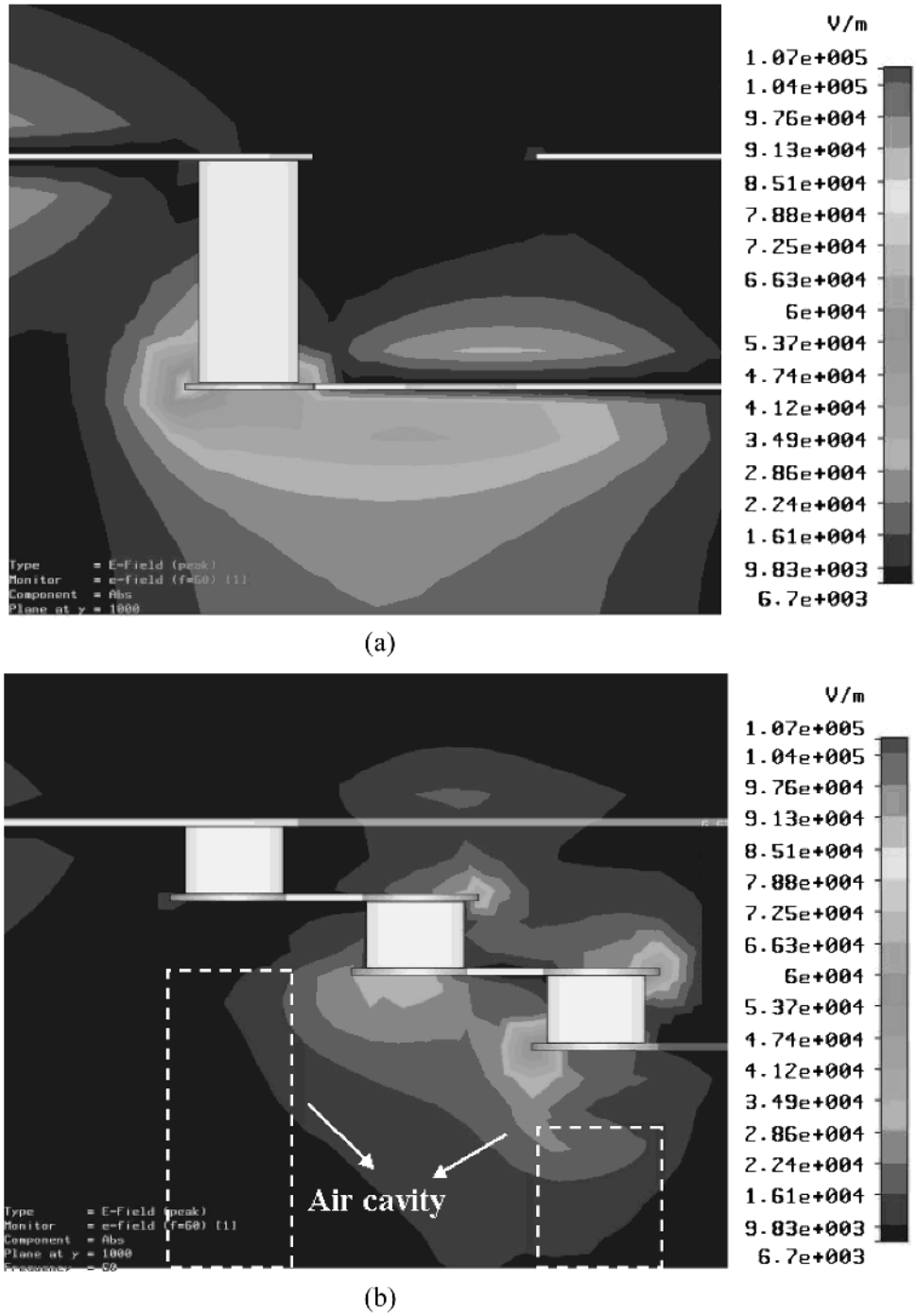

Fig. 4. Cross-sectional view of the electric field distribution of two CPW-to-SL vertical via transitions at 60 GHz. (a) Conventional transition. (b) Novel transition.

tric field results of Fig. 4, its input impedance is much better matched to 50 Ω than that with the conventional one from 50 to 65 GHz and 1-dBimprovement of the insertion loss (S21) is observed at 60 GHz. These improved characteristics result from much smaller parasitics due to the STV structure and embedded air cavities than the conventional one.

Noting that electric fields are confined and transmission characteristics are improved in the novel STV transition embedding air cavities. This can be explained by analyzing the maximum dimension and discontinuity of the vertical via. The transmission characteristics of the vertical transition are degraded, because the maximum dimension of the vertical vias block is much larger than λ_{op}. In the conventional vertical transition [12], [13] using three vias stacked directly, the total height is 300 μm, and its rate to λ_{op} is 11%. Here, λ_{op} on the LTCC CPW is 2.56 mm at 60 GHz. Using the proposed STV structure, the conventional stacked vias are subdivided into vias of very small height (relative to the λ_{op}); therefore, the rate to λ_{op} can be decreased from 11% to 3.9%. However, additional shunt capacitance due to the STV structure can lead to a leakage path and signal propagation delay. Therefore, the parasitic capacitance needs to be reduced. An equivalent relative permittivity [14] between transition vias

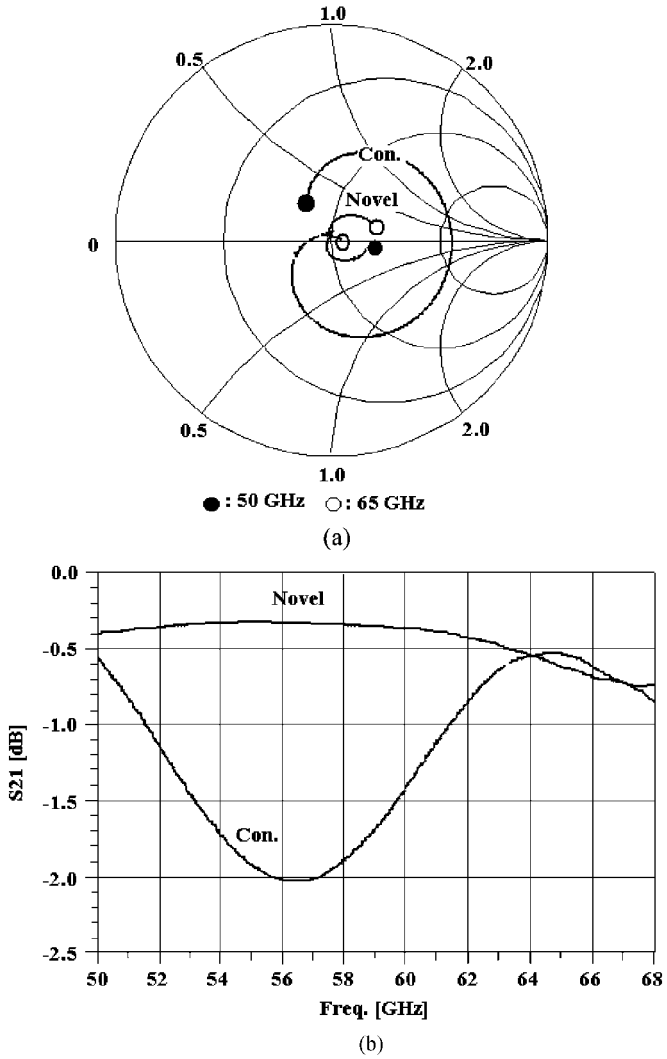

Fig. 5. Simulated transmission coefficients of three-segment transmission lines using the novel vertical transition and the conventional one. (a) Return losses (S11). (b) Insertion losses (S21).

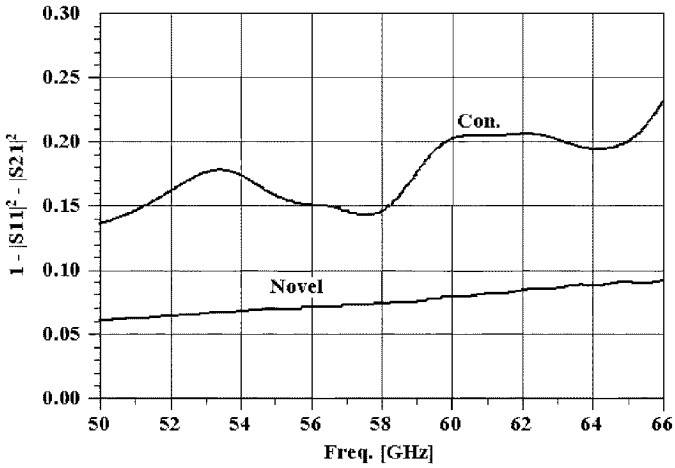

Fig. 6. Calculated radiation losses of three-segment transmission lines using the novel vertical transition and the conventional one.

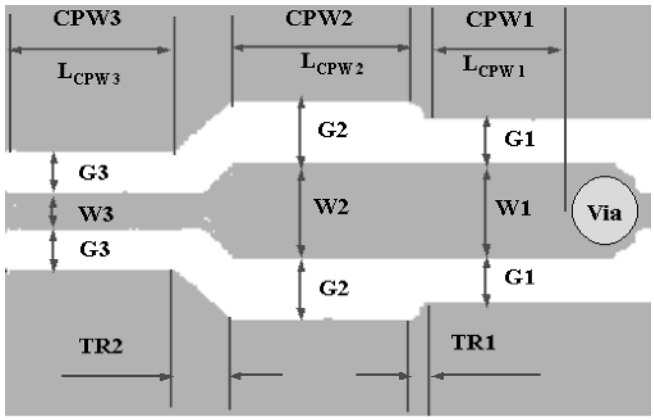

Fig. 7. Two CPW-to-CPW planar transitions (W2 = 244 μm, W3 = 100 μm, G2 = 140 μm, G3 = 90 μm, TR1 = 40 μm, TR2 = 144 μm, LCPW1 = 500 μm, LCPW2 = 430 μm, and LCPW3 = 500 μm).

with air cavities and the ground plane is drastically decreased from 7.0 to 1.4 due to embedded air cavities; its reduction rate is ~80%, Consequently, the parasitic shunt capacitance is reduced markedly.

For quantitative analysis of potential improved performance, radiation losses [15] $(1 - |S11|^2 - |S21|^2)$ of two three-segment lines are calculated from the simulated transmission coefficients. In the novel case, its radiation shows less than 10 % at the all simulated frequencies as shown in Fig. 6. The novel one achieves an improvement of 62% in radiation. This value matches well to the estimated value.

B. CPW-to-CPW Planar Transition

The CPW-to-CPW planar transitions are also designed for reduction of ground plane discontinuity which results from the difference in height between the BPF and active device ground planes as shown in Fig. 2. The SL structured BPF using six layers has a ground height of 600 μm. In contrast, that of a MMIC mounted in a cavity is 100 μm. This steep difference of ground plane height can cause radiation problems. Therefore, the signal line is on the same seventh layer, but ground planes are transited gradually from the first layer to the third and fifth layers using internal ground planes, as shown in Fig. 2. According to different ground plane heights, there are three sections of CPWs and two transitions (TR1 and TR2) among them, as shown in Fig. 7. Their width and the gap for 50-Ω impedance-CPW lines are designed.

In order to verify the proposed vertical and planar transition, we designed and fabricated a seven-segment transmission line (CPW3–CPW2–CPW1–SL–CPW1–CPW2–CPW3) using the standard LTCC process. The air cavities were of the same shape as the signal vias, but they were not filled with metal. Fig. 8 shows the fabricated seven-segment transmission line involving two planar transitions and one vertical transition at each end of the transmission line. The length of a SL is 2000 μm, and the total length of CPW-to-CPW transition is 1430 μm.

Fig. 9 shows measured results of the fabricated transition. An insertion loss shows flat value of -1.6 dB from 50 to 60 GHz. The input and output return losses are below -15 dB from 52 to 62 GHz. In particular, those at the operation frequency band are below -20 dB. Considering the total losses of all transmission lines (six CPWs and a SL) of -0.37 dB, which is calculated by

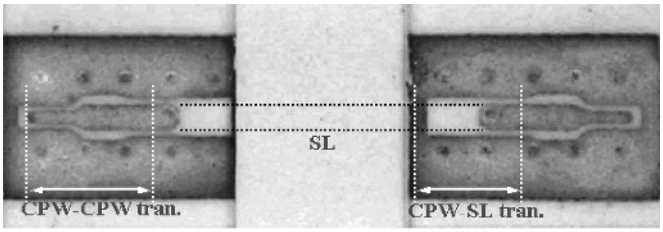

Fig. 8. Fabricated three-segment transmission lines using vertical and planar transitions.

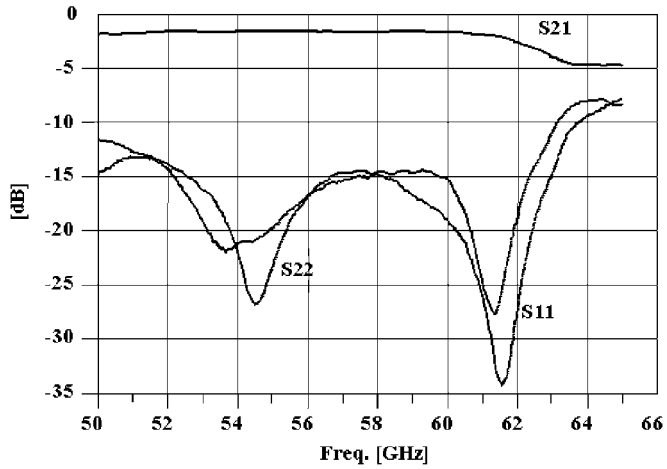

Fig. 9. Measured results of the fabricated transition.

a conventional line calculator, the transition loss is 0.62 dB per an STV vertical and a planar transition at 60 GHz.

C. Embedded Stripline BPF

A dual-mode four-pole BPF is designed in between the L2 and L7 layer using dual-mode patch resonators [12] as shown in Fig. 2. The dual mode can be generated from a single resonator by adding a perturbation (cut) at a point that is 45° from the axes of coupling to the resonator [12] as shown in Fig. 10. It enables two orthogonal modes, which are generated in the resonator, to be coupled. Because the side length of each square patch is about half a wavelength, there are no narrow lines, the width of which is close to process limitations. Therefore, such a resonator has reduced process sensitivity.

The target of the embedded SL BPF is to realize a 3-dB bandwidth (BW) of 3.3 % at the center frequency of 60.4 GHz. This filter has to achieve LO rejection over 20 dBc at 58 GHz (the LO frequency). The side length of a resonator is about half a wavelength (623 μm) [16]. The widths of the feed lines are 135 μm. Changing the depth of the cut, coupling coefficients can be controlled, and an optimum cut length is calculated as 150 μm.

For good skirt characteristics, two resonators are on the third and fifth layers, and two of their blocks are 684 μm away from each other for four-pole operation, as shown in Fig. 10. Feed lines, external coupling between the resonators on the third and fifth layers, and internal coupling between their two blocks are on the fourth layer. The external coupling distances on the fourth layer are 140 μm, and the internal coupling is realized by an overlap of 40 μm between two resonators on the third and fifth layer.

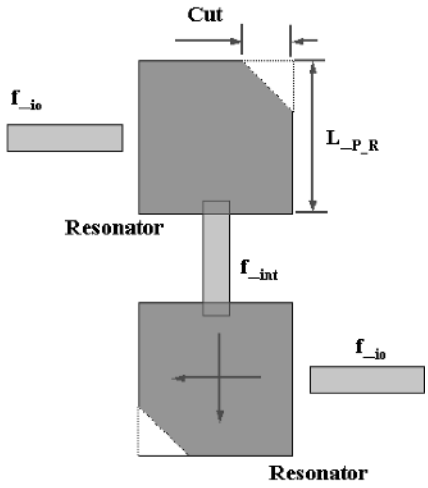

Fig. 10. Layout of a BPF using the dual-mode patch resonator (L_{P_R}: the length of a patch resonator, and Cut: the cutting length).

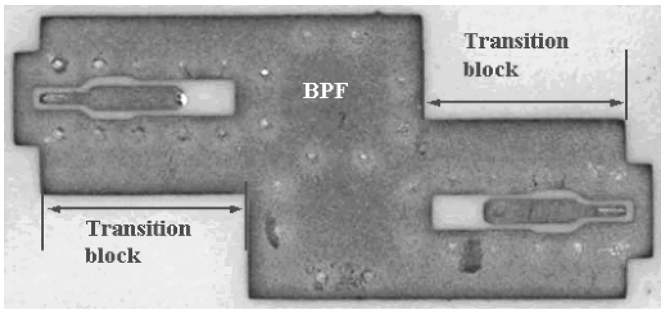

Fig. 11. Fabricated 60-GHz LTCC stripline BPF ($3.2 \times 6.5 \times 0.7$ mm^3).

III. Fabrication and Measured Performance

The designed BPF was implemented in seven LTCC dielectric layers using a standard LTCC process. Fig. 11 shows the fabricated BPF and its total size of the fabricated BPF including whole transitions was 3.2 mm $\times$ 6.5 mm $\times$ 0.7 mm, where the areas occupied by the filter and the transition are 1.8×3.5 mm^2 and 2.4×0.9 mm^2, respectively.

In Fig. 12, the comparison of the simulated and measured results is presented. The measurement shows a higher center frequency (f_c) and narrower bandwidth (BW) than the simulation results. This is owing to misalignment among the multilayer dielectrics. Our LTCC process offers $a \pm 20$ μm align tolerance. The misalignment among the layers, on which the feed lines and the resonators were screen-printed, results in varying the coupling coefficients. Therefore, the measured frequency characteristics are slightly different from the simulated results. The measured f_c and BW are 60.4 GHz and 3.5%, respectively. The return losses are below -15 dB at the pass band. The LO rejection is 20.5 dBc at 58 GHz. The insertion loss including the transitions is 5.27 dB. Considering the insertion loss of the transitions, the filter insertion loss is 4.0 dB.

IV. Conclusion

A novel SL structured BPF integrating air cavities has been proposed and implemented for 60-GHz LTCC SiP applications. For low-loss interconnection with active devices a novel transition including a CPW-to-SL vertical via and CPW-to-CPW

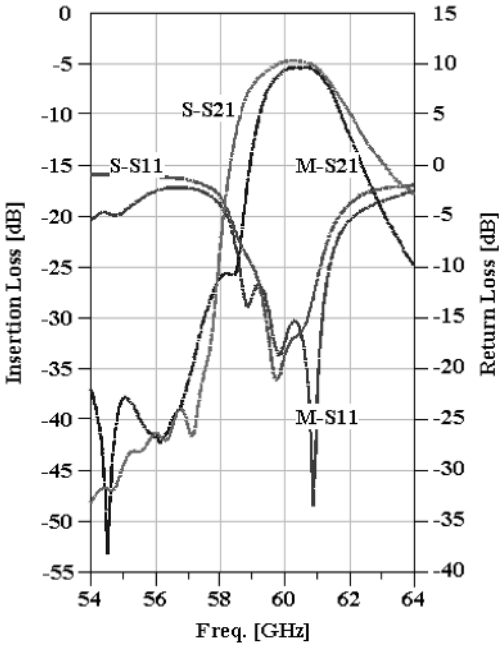

Fig. 12. Simulated and measured performances of the 60 GHz LTCC SL BPF (S-: simulated, and M-: measured).

planar transition is devised using the stagger via (STV) structure and embedded air cavities. Using the 3-D EM analysis, proposed transition structures demonstrate to reduce radiation due to discontinuities. The fabricated seven-segment transmission line (CPW3–CPW2–CPW1–SL–CPW1–CPW2–CPW3) composed of the two CPW-to-SL transitions and four CPW-to-CPW planar transitions achieves an insertion loss of 1.6 dB and return losses below −20 dB at the passband of the filter. The transition loss (one vertical and two planar transitions) except transmission lines is 0.62 dB at 60 GHz. Adopting the novel vertical transition, the four-pole SL BPF is designed and fabricated. The LTCC BPF achieves 3.5 % bandwidth at the center frequency of 60.4 GHz. Its return losses are below −15 dB at the passband, and its insertion loss is 4.0 dB.

REFERENCES

[1] K. Ohata, K. Maruhashi, M. Ito, S. Kishimoto, K. Ikuina, T. Hashiguchi, K. Ikeda, and N. Takahashi, "1.25 Gbps wireless gigabit Ethernet link at 60-GHz band," in *Proc. IEEE MTT-S Int. Microw. Symp. Dig.*, Jun 2003, vol. 1.1, pp. 373–376.

[2] A. Yamada, E. Suematsu, K. Sato, M. Yamamoto, and H. Sato, "60 GHz ultra compact transmitter/receiver with a low phase noise PLL-oscillator," in *Proc. IEEE MTT-S Int. Microw. Symp. Dig.*, Jun. 2003, vol. 3, pp. 2035–2038.

[3] Y. C. Lee, W.-I. Chang, Y. H. Cho, and C. S. Park, "A very compact 60 GHz transmitter integrating GaAs MMICs on LTCC passive circuits for wireless terminal applications," in *Proc. IEEE Compound Semiconductor Integrated Circuit Symp. Technical Dig.*, Oct. 2004, pp. 313–316.

[4] Y. C. Lee, W.-I. Chang, and C. S. Park, "Monolithic LTCC SiP transmitter for 60 GHz wireless communication terminals," in *Proc. IEEE MTT-S Int. Microw. Symp. Dig.*, Jun. 2005, pp. 1015–1018.

[5] P. Blondy, A. R. Brown, and G. M. Rebeiz, "Low-loss micromachined filters for millimeter-wave communication systems," *IEEE Trans. Microw. Theory Tech.*, vol. 46, no. 12, pp. 2283–2288, Dec. 1998.

[6] M. Ito, K. Maruhashi, K. Ikuina, T. Hashiguchi, S. Iwanaga, and K. Ohata, "A 60-GHz-band planar dielectric waveguide filter for flip-chip modules," *IEEE Trans. Mircrow. Theory Techn.*, vol. 49, no. 12, pp. 2431–2436, Dec. 2001.

[7] J. A. Curtis and S. J. Fiedziuszko, "Miniature dual mode microstrip filters," in *Proc. IEEE MTT-S Int. Microw. Symp. Dig.*, 1991, pp. 443–446.

[8] Y. C. Lee and C. S. Park, "A new millimeter-wave stripline resonator with embedded air cavities in LTCC multilayer structure," in *Proc. IEEE MTT-S Int. Microw. Symp. Dig.*, 2003, vol. 3, pp. 2027–2030.

[9] Y. C. Lee and C. S. Park, "Novel low-loss LTCC microstrip lines with air cavities embedded in the LTCC substrate," in *Proc. IEEE Asia Pacific Microw. Conf. (APMC)*, 2003, vol. 3, pp. 1511–1514.

[10] Y. C. Lee and C. S. Park, "A novel high-Q LTCC stripline resonator for millimeter-wave applications," *IEEE Microw. Wireless Compon. Lett.*, vol. 13, no. 12, pp. 499–501, Dec. 2003.

[11] CST Microwave Studio. CST, Inc. [Online]. Available: http://www.cst.com

[12] F. J. Schmuckle, A. Jentzch, W. Heinrich, J. Butz, and M. Spinnler, "LTCC as MCM substrate: Design of strip-line structures and flip-chip interconnections," in *Proc. IEEE MTT-S Int. Microw. Symp. Dig.*, 2001, vol. 3, pp. 1093–1096.

[13] A. Panther, C. Glaser, M. G. Stubbs, and J. S. Wight, "Vertical transitions in low temperature co-fired ceramics for LMDS applications," in *Proc. IEEE MTT-S Int. Microw. Symp. Dig.*, 2001, vol. 3, pp. 1907–1910.

[14] S. G. Cigdem and Y. Erdem, "New computation of the resonant frequency of a tunable equilateral triangular microstrip patch," *IEEE Trans. Microw. Theory Tech.*, vol. 48, no. 3, pp. 334–338, Mar. 2000.

[15] S. Lee and M. Hayakawa, "A study on the radiation loss from a bent transmission line," *IEEE Trans. Electromagn. Compat.*, vol. 43, no. 4, pp. 618–621, Nov. 2001.

[16] I. J. Bahl and P. Bhartia, *Microstrip Antennas*. Norwood, MA: Artech House, 1982.

Young Chul Lee (M'06) received the B.S. and M.S degrees in electronic engineering from Yeungnam University, Gyeongsan, Korea, in 1995 and 1997, respectively, and the Ph.D. degree in electronic engineering from Information and Communications University (ICU), Daejeon, Korea, in 2005.

From 1997 to 2000, he was with the R&D Division, LG Semicon, Inc., Cheongju, Korea, where he was involved in the development of MOSFET devices for DRAM applications. In 2005, he joined Mokpo National Maritime University (MMU), Mokpo, Korea, as an Assistant Professor in the Division of Marine Electronics and Communication Engineering. His professional interests are millimeter-wave circuits and systems, 3-D integration of RF circuits using LTCC-based system-in-package (SiP) technology, and reconfigurable RF circuits.

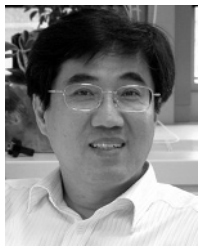

Chul Soon Park (M'97) received the B.S. degree in metallurgical engineering from Seoul National University, Seoul, Korea, in 1980 and the M.S. and Ph.D. degrees in materials science from the Korea Advanced Institute of Science and Technology (KAIST), Daejeon, in 1982 and 1985, respectively.

From 1985 to 1999, he was with the Electronics and Telecommunication Research Institute (ETRI), Daejeon, where he contributed to development of semiconductor devices and circuits. From 1987 to 1989, he studied the very initial growth of group IV semiconductors during the visit to the AT&T Bell Laboratories, Murray Hill, NJ. Since 1999, he has been with the Information and Communications University (ICU), Daejeon, Korea, where he is a Professor in the Engineering School and the Director of the Intelligent Radio Engineering Center. His research focuses on the power amplifier, reconfigurable RFICs, and their SoC/SoP integration.